Atmos. Chem. Phys., 11, 583–598, 2011
www.atmos-chem-phys.net/11/583/2011/
doi:10.5194/acp-11-583-2011

Atmospheric Chemistry and Physics

Formation of secondary aerosols over Europe: comparison of two gas-phase chemical mechanisms

Y. Kim, K. Sartelet, and C. Seigneur

CEREA, Joint Laboratory École des Ponts ParisTech/EDF R&D, Université Paris-Est, 77455 Champs sur Marne, France

Received: 13 August 2010 – Published in Atmos. Chem. Phys. Discuss.: 31 August 2010
Revised: 9 November 2010 – Accepted: 5 January 2011 – Published: 20 January 2011

Abstract. The impact of two recent gas-phase chemical kinetic mechanisms (CB05 and RACM2) on the formation of secondary inorganic and organic aerosols is compared for simulations of $PM_{2.5}$ over Europe between 15 July and 15 August 2001. The host chemistry transport model is Polair3D of the Polyphemus air-quality platform. Particulate matter is modeled with a sectional aerosol model (SIREAM), which is coupled to the thermodynamic model ISORROPIA for inorganic species and to a module (MAEC) that treats both hydrophobic and hydrophilic species for secondary organic aerosol (SOA). Modifications are made to the gas-phase chemical mechanisms to handle the formation of SOA. In order to isolate the effect of the original chemical mechanisms on PM formation, the addition of reactions and chemical species needed for SOA formation was harmonized to the extent possible between the two gas-phase chemical mechanisms. Model performance is satisfactory with both mechanisms for speciated $PM_{2.5}$. The monthly-mean difference of the concentration of $PM_{2.5}$ is less than $1\,\mu g\,m^{-3}$ (6%) over the entire domain. Secondary chemical components of $PM_{2.5}$ include sulfate, nitrate, ammonium and organic aerosols, and the chemical composition of $PM_{2.5}$ is not significantly different between the two mechanisms. Monthly-mean concentrations of inorganic aerosol are higher with RACM2 than with CB05 (+16% for sulfate, +11% for nitrate, and +10% for ammonium), whereas the concentrations of organic aerosols are slightly higher with CB05 than with RACM2 (+22% for anthropogenic SOA and +1% for biogenic SOA). Differences in the inorganic and organic aerosols result primarily from differences in oxidant concentrations (OH, O_3 and NO_3). Nitrate formation tends to be HNO_3-limited over land and differences in the concentrations of nitrate are due to differences in concentration of HNO_3. Differences in aerosols formed from aromatic SVOC are due to different aromatic oxidation between CB05 and RACM2. The aromatic oxidation in CB05 leads to more cresol formation, which then leads to more SOA. Differences in the aromatic aerosols would be significantly reduced with the recent CB05-TU mechanism for toluene oxidation. Differences in the biogenic aerosols are due to different oxidant concentrations (monoterpenes) and different particulate organic mass concentrations affecting the gas-particle partitioning of SOA (isoprene). These results show that the formulation of a gas-phase chemical kinetic mechanism for ozone can have significant direct (e.g., cresol formation) and indirect (e.g., oxidant levels) effects on PM formation. Furthermore, the incorporation of SOA into an existing gas-phase chemical kinetic mechanism requires the addition of reactions and product species, which should be conducted carefully to preserve the original mechanism design and reflect current knowledge of SOA formation processes (e.g., NO_x dependence of some SOA yields). The development of chemical kinetic mechanisms, which offer sufficient detail for both oxidant and SOA formation is recommended.

1 Introduction

The contribution of secondary aerosols formed from atmospheric gas-phase species to the total amount of particulate matter (PM) is important in many urban and remote areas (Seinfeld and Pandis, 1998; Finlayson-Pitts and Pitts Jr., 2000). In particular, secondary aerosols dominate atmospheric PM in Europe at many monitoring sites (Putaud et al., 2010). Secondary aerosols consist of inorganic and organic components. The formation of secondary aerosols is due to various physical processes (nucleation, condensation and evaporation) and chemical processes (photochemical gas-phase oxidation leading to the formation of semi-volatile

Correspondence to: Y. Kim
(kimy@cerea.enpc.fr)

products that may condense onto particles, aqueous-phase oxidation and particulate-phase processes).

Hence the gas-phase chemical mechanisms in air quality models (AQMs) play an important role in modeling aerosol concentrations. Different gas-phase chemical kinetic mechanisms have been developed to represent atmospheric chemistry, ranging from simple (less than ten species) to complex (several thousand species). Condensed mechanisms with 50 to 100 species (e.g., SAPRC (Carter, 2000, 2010), RACM (Stockwell et al., 1997; Goliff and Stockwell, 2008) and carbon-bond mechanisms (Gery et al., 1989; Yarwood et al., 2005)) are typically used in three-dimensional (3-D) AQMs to simulate the evolution of ozone and PM. Condensed mechanisms are classified as lumped structure mechanisms (carbon-bond mechanisms: CB05 and CBM-IV) and lumped species mechanisms (e.g., SAPRC and RACM mechanisms).

Several studies have been carried out to understand the impact of the gas-phase chemical mechanism on the formation of secondary aerosols. Sarwar et al. (2008) compared CB05 and CBM-IV for the formation of sulfate, nitrate and secondary organic aerosol (SOA) using the Community Multiscale Air Quality model (CMAQ). Luecken (2008) compared the impact of CB05, CBM-IV and SAPRC99 on $PM_{2.5}$ (particles less than 2.5 µm in aerodynamic diameter) for regulatory applications in the United States. Pan et al. (2008) compared CBM-Z, CB05 and SAPRC99 for the formation of inorganic PM using the Weather Research and Forecasting model coupled with Chemistry (WRF/Chem) and the Model of Aerosol Dynamics, Reaction, Ionization, and Dissolution 1 (MADRID 1).

This study focuses on differences in $PM_{2.5}$ concentrations over Europe simulated with two recent chemical mechanisms, a carbon-bond mechanism, CB05, and a lumped species mechanism, RACM2. The gas-phase mechanisms were incorporated within Polair3D, the 3-D AQM of the Polyphemus air-quality platform (Kim et al., 2009). First, a brief description of the model used in this study is given. Coupling between the aerosol model and the chemical mechanisms is then discussed. Next, the setup of the simulations is described and simulation results are compared to observed data. To analyze the impact of the gas-phase chemical mechanism on PM concentrations, the chemical composition of $PM_{2.5}$ over Europe is presented in the first part of the analysis. Then, mean concentrations of inorganic and organic $PM_{2.5}$ simulated with CB05 and RACM2 are compared over the whole domain for each chemical component. Next, comparisons of the spatial distributions of aerosols are presented. The results are discussed in a diagnostic manner to identify the main causes of the discrepancies.

2 Model descriptions

The chemistry transport model Polair3D (Sartelet et al., 2007) of the air-quality platform Polyphemus version 1.6 (Mallet et al., 2007) is used in this study (http://cerea.enpc.fr/polyphemus). PM is modeled with SIREAM (SIze REsolved Aerosol Model). SIREAM segregates the particle size distribution into sections and simulates nucleation, coagulation and condensation/evaporation processes (Debry et al., 2007a). SIREAM is coupled to the thermodynamic model ISORROPIA for inorganic species (Nenes et al., 1998).

2.1 SOA module

The SOA Modified AER/EPRI/Caltech module (MAEC) calculates the secondary organic components of particles (Debry et al., 2007b). MAEC is based on the AEC model of Pun et al. (2002, 2006). Precursors of SOA in the model include anthropogenic compounds (aromatics, long-chain alkanes and long-chain alkenes) and biogenic compounds (isoprene, monoterpenes, and terpenoids). This model includes an explicit treatment of hydrophilic SOA species. As described by Pun et al. (2002), condensable oxidation products of VOC are grouped into two categories: hydrophobic compounds, which can be absorbed into organic particles and hydrophilic compounds, which can be absorbed into aqueous particles (typically inorganic particles containing sulfate, ammonium and possibly nitrate). When the relative humidity is very low and no aqueous particles are present, hydrophilic compounds may be absorbed into organic particles. Those condensable oxidation products are represented by a limited number of surrogate SOA species, which are selected to represent the ensemble of possible SOA species. Those surrogate SOA species are selected based on the SOA molecular constituents identified in smog chamber experiments for monoterpene precursors and their physico-chemical properties such as their octanol/water partitioning coefficient (to determine whether they are hydrophobic or hydrophilic), their saturation vapor pressure (for both hydrophobic and hydrophilic SOA species) and their dissociative properties in aqueous solutions (for hydrophilic SOA species) (see Pun et al. (2006) for details on the method for selecting SOA surrogates). Because less information on the molecular constituents of SOA is available for products of anthropogenic precursors, the surrogate SOA species were selected based on SOA molecular species derived from a theoretical chemical mechanism of the precursor oxidation (e.g., Griffin et al., 2002).

Table 1 summarizes the surrogate SOA species, their precursors, and their physico-chemical properties used in the model. For isoprene, the representation of Zhang et al. (2007) was used. Absorption of SOA into organic particles follows Raoult's law and depends on the average molecular weight of the organic particulate mixture, the saturation vapor pressure of the condensing SOA surrogate and its activity

Table 1. Surrogate SOA compounds, their corresponding precursors and their physico-chemical properties.

Precursors	Surrogate SOA species[a]	Molecular weight ($g\,mole^{-1}$)	Saturation vapor pressure (Pa)	Henry's law constant[b] ($\mu g/\mu g$ water)/($\mu g/m^3$ air)	Enthalpy of vaporization ($kJ\,mole^{-1}$)
Anthropogenic compounds (aromatics, long-chain alkanes and alkenes)	AnBmP	152	4.0×10^{-4}	NA	88
	AnBlP	167	2.7×10^{-7}	NA	88
	AnClP	167	2.7×10^{-7}	NA	88
Biogenic compounds (monoterpenes and terpenoids)	BiA0D	168	3.6×10^{-2}	4.82×10^{-5}	88
	BiA1D	170	2.9×10^{-5}	2.73×10^{-3}	88
	BiA2D	186	1.9×10^{-5}	6.25×10^{-3}	109
	BiBmP	236	4.0×10^{-5}	NA	175

[a] The SOA surrogate nomenclature is as follows. First two letters: An = anthropogenic, Bi = biogenic; third letter: A: hydrophilic, B: hydrophobic, C: hydrophobic formed under low-NO_x conditions (see text); last two characters: 2D = twice dissociative, 1D = once dissociative, 0D = non-dissociative for hydrophilic compounds; lP = low saturation vapor pressure, mP = moderate saturation vapor pressure for hydrophobic compounds.
[b] NA: not applicable for hydrophobic compounds.

coefficient in the particle. Absorption of hydrophilic SOA into aqueous particles follows Henry's law and depends on the liquid water content of the particle, its pH (for mono- and dicarboxylic acids, i.e., BiA1D and BiA2D, respectively) and the activity coefficients of the dissolved species. Activity coefficients of organic compounds are calculated for both the organic phase and the aqueous phase using UNIFAC (see Pun et al. (2002) for details regarding the computational implementation of the gas/particle partitioning and activity calculations).

Oligomerization is represented according to the pH-dependent parametrization of Pun and Seigneur (2007), which applies to aqueous-phase oxo-SOA (i.e., BiA0D). In addition, it is assumed that glyoxal and methylglyoxal can oligomerize and thereby contribute to SOA formation; following Pun and Seigneur (2007), empirical gas/particle partitioning coefficients were used to that end (9.1×10^{-6} ($\mu g/\mu g$ water)/($\mu g/m^3$ air) for glyoxal and 5.6×10^{-12} ($\mu g/\mu g$ water)/($\mu g/m^3$ air) for methylglyoxal).

A major difference with previous work is the NO_x-dependency for SOA formation from aromatic compounds. Ng et al. (2007) showed that the SOA yields from aromatic oxidation were greater under low-NO_x conditions than under high-NO_x conditions. Accordingly, different yields are used for SOA formation under those different regimes with two surrogates being used for the high-NO_x regimes (AnBmP and AnBlP) and one surrogate being used for the low-NO_x regime (AnClP). To properly account for different yields for different NO_x regimes, SOA formation is not treated as a product of the first oxidation step of the VOC precursor, but instead it is treated in later oxidation steps as discussed in Sect. 2.2.

2.2 Chemical kinetic mechanisms

RACM2 (Goliff and Stockwell, 2008, 2010) is a recent mechanism developed via various improvements in RACM (Stockwell et al., 1997). Recent developments in RACM2 related to aerosol formation concern the benzene scheme, separation of xylene isomers (XYO for o-xylene and XYL for m- and p-xylene) and glyoxal photolysis. For the benzene scheme, phenol is now explicitly speciated as a product of benzene oxidation (Goliff and Stockwell, 2010). This speciation of phenol is important because the oxidation of phenol leads to the formation of aromatic compounds, which are SOA precursors (Pun and Seigneur, 2007).

CB05 (Yarwood et al., 2005) is an updated version of CBM-IV (Gery et al., 1989). In CB05, most organic compounds are divided into smaller species elements based on the bond types of their carbon atoms.

Kim et al. (2009) studied the impact of using either CB05 or RACM2 on the chemistry of ozone formation over Europe. This work focuses on aerosol formation. To couple the chemical kinetic mechanisms with the aerosol module MAEC, gas-phase organic precursors of SOA in CB05 and RACM2 were modified or added as described in Sect. 2.3.

Furthermore, the dinitrogen pentoxide (N_2O_5) chemistry in CB05 was modified. The concentration of N_2O_5 does not strongly impact ozone formation chemistry, but it is important for the formation of particulate nitrate via heterogeneous chemistry (Jacob, 2000). CB05 involves two gas-phase reactions of N_2O_5 with water; one is a bimolecular reaction and the other is a termolecular reaction. Following the recent recommendation of IUPAC (International Union of Pure and Applied Chemistry), we excluded the termolecular reaction from CB05 and set an upper limit of $1.0 \times 10^{-22}\,cm^3\,molecule^{-1}\,s^{-1}$ for the bimolecular reaction rate coefficient in the two mechanisms (www.iupac-kinetic.ch.cam.ac.uk).

Table 2. Gas-phase organic precursors in the two mechanisms.

Precursor type	RACM	CB05
Aromatics	TOL, XYL, XYO, CSL, PHEN	TOL, XYL, CRES
Alkanes	HC8	HC8*
Anthropogenic alkenes	OLT, OLI	OLE, IOLE
Biogenic alkenes	API, LIM, ISO	API*, LIM*, ISOP

* added surrogates.

2.3 SOA formation in CB05 and RACM2

As organic gases are oxidized in the gas phase by hydroxyl radicals (OH), ozone (O_3) and nitrate radicals (NO_3), their volatility evolves. Their volatility may decrease by the addition of polar functional groups (such as hydroxyl, hydroperoxyl, nitrate and acid groups). On the other hand, oxidation products may have higher volatility than the parent organic gases due to the cleavage of carbon-carbon bonds. Products of low volatility may condense on the available particles to establish equilibrium between the gas and particle phases. There are four types of gas-phase organic precursors treated in MAEC: aromatics, long-chain alkanes, long-chain anthropogenic alkenes and biogenic alkenes. These precursors are consistent with the RACM2 species because MAEC was originally developed in conjuction with RACM (Debry et al., 2007b). However, some of these precursors are not available in CB05 and it is necessary to add them to make CB05 compatible with MAEC. These additions are made in such a way that they do not affect CB05 for oxidant formation. Table 2 summarizes the gas-phase organic precursors for CB05 and RACM2. The gas-phase organic precursors are oxidized to form Semi-Volatile Organic Compound (SVOC), which may condense onto particles.

For aromatic precursors, RACM2 includes two surrogates (XYO, XYL) for xylenes, whereas CB05 includes only one surrogate (XYL) for all xylene isomers. Phenol is explicitly modeled in RACM2 with the PHEN surrogate species. The two mechanisms have the same precursors for toluene and cresols. RACM2 represents long-chain alkane precursors with the HC8 surrogate species, which represents alkanes with an OH rate constant greater than $6.8 \times 10^{-12}\,\mathrm{cm^3\,molecule^{-1}\,s^{-1}}$. CB05 does not explicitly include any alkane surrogate to form SOA because alkane species are decomposed into PAR elements, which is the single carbon-bond surrogate. Therefore, it is necessary to add a supplementary species to take into account the effect of alkanes on SOA formation in CB05. Here, we add the HC8 surrogate of RACM2 to the CB05 mechanism. The two mechanisms have the same anthropogenic alkene precursors, but biogenic alkene precursors differ. Monoterpenes are represented with two species, API (α-pinenes and other cyclic terpenes with one double bond) and LIM (d-limonene and other cyclic diene-terpenes), in RACM2 but only one species, TERP, in CB05. Because MAEC was developed originally using surrogate species of RACM (Debry et al., 2007b), biogenic SOA are formed from the two species API and LIM. To have a similar treatment of SOA formation by monoterpenes in CB05, API and LIM are added to CB05 for biogenic SOA formation, in parallel to TERP, which is used solely for the gas-phase chemistry.

Tables 3a and 3b present the toluene and xylene oxidation chemistry, respectively, for SVOC formation in CB05 and RACM2. For toluene and xylene, we differentiate the oxidation under low-NO_x and high-NO_x conditions. Under low-NO_x conditions, SVOC are formed from the oxidation of peroxy radicals formed from toluene or xylenes by HO_2, methyl-peroxy radical or higher peroxy radical surrogates (carbon number ≥ 2), whereas under high-NO_x conditions, SVOC are formed from the oxidation of those toluene or xylene peroxy radicals with NO and NO_3. New reactions to model the formation of SVOC by the oxidation of toluene and xylene peroxy radicals are added to both CB05 and RACM2. In these reactions, the oxidants are also added as product of the reactions, so that oxidant formation is not affected by SVOC formation.

The SVOC formation chemistry for other aromatic precursors (cresol and phenol) is similar between CB05 and RACM2 even though only RACM2 explicitly includes phenol. We assume that the yield of SVOC from phenol is analogous to the yield of SVOC from cresol (Pun and Seigneur, 2007). Table 3c presents the cresol and phenol oxidation chemistry.

For long-chain alkanes and anthropogenic alkenes, the two mechanisms have the same oxidation chemistry. Table 3d presents the long-chain alkane and anthropogenic alkene oxidation chemistry.

The oxidation chemistry of biogenic alkenes (monoterpenes and isoprene) is presented in Table 3e. As mentioned above, the monoterpene surrogates API and LIM of RACM2 were added to CB05, as well as the reactions in which they are involved for the SVOC formation. In these reactions, the oxidants are also added as products of the reactions, so that the original gas-phase mechanism is not affected by SVOC formation.

Table 3a. Toluene oxidation chemistry for SVOC formation.

RACM2	CB05
TOL + HO → 0.25 TOLPAEC[a] + other products	TOL + OH → 0.25 TOLPAEC[a] + other products
TOLPAEC + HO2 → 0.78 AnClP + HO2[b]	TOLPAEC + HO2 → 0.78 AnClP + HO2[b]
TOLPAEC + MO2 → 0.78 AnClP +MO2[b]	TOLPAEC + MEO2 → 0.78 AnClP + MEO2[b]
TOLPAEC + ACO3 → 0.78 AnClP + ACO3[b]	TOLPAEC + C2O3 → 0.78 AnClP + C2O3[b]
TOLPAEC + NO → 0.053 AnBlP + 0.336 AnBmP + NO[b]	TOLPAEC + NO → 0.053 AnBlP + 0.336 AnBmP + NO[b]
TOLPAEC + NO3 → 0.053 AnBlP + 0.336 AnBmP + NO3[b]	TOLPAEC + NO3 → 0.053 AnBlP + 0.336 AnBmP + NO3[b]

[a] new peroxy radical formed from toluene.
[b] oxidant species added as a product to retain the original gas-phase mechanism, new reactions added to both RACM2 and CB05 mechanisms for the SVOC formation.

Table 3b. Xylenes oxidation chemistry for SVOC formation.

RACM2	CB05
XYL + HO → 0.274 XYLPAEC[a] + other products	XYL + OH → 0.274 XYLPAEC[a] + other products
XYLPAEC + HO2 → 0.71 AnClP + HO2[b]	XYLPAEC + HO2 → 0.71 AnClP + HO2[b]
XYLPAEC + MO2 → 0.71 AnClP + MO2[b]	XYLPAEC + MEO2 → 0.71 AnClP + MEO2[b]
XYLPAEC + ACO3 → 0.71 AnClP + ACO3[b]	XYLPAEC + C2O3 → 0.71 AnClP + C2O3[b]
XYLPAEC + NO → 0.023 AnBlP + 0.32 AnBmP + NO[b]	XYLPAEC + NO → 0.023 AnBlP + 0.32 AnBmP + NO[b]
XYLPAEC + NO3 → 0.023 AnBlP + 0.32 AnBmP + NO3[b]	XYLPAEC + NO3 → 0.023 AnBlP + 0.32 AnBmP + NO3[b]
XYO + HO → 0.274 XYOPAEC[a] + other products	
XYOPAEC + HO2 → 0.71 AnClP + HO2[b]	
XYOPAEC + MO2 → 0.71 AnClP + MO2[b]	
XYOPAEC + ACO3 → 0.71 AnClP + ACO3[b]	
XYOPAEC + NO → 0.023 AnBlP + 0.32 AnBmP + NO[b]	
XYOPAEC + NO3 → 0.023 AnBlP + 0.32 AnBmP + NO3[b]	

[a] new peroxy radicals formed from xylenes.
[b] see Table 3a.

Table 3c. Cresol and phenol oxidation chemistry for SVOC formation.

RACM2	CB05
CSL* + HO → 0.014 AnBlP + 0.09 AnBmP + other products	CRES* + OH → 0.014 AnBlP + 0.09 AnBmP + other products
CSL + NO3 → 0.04 AnBlP + 0.12 AnBmP + other products	CRES + NO3 → 0.04 AnBlP + 0.12 AnBmP + other products
PHEN + HO → 0.014 AnBlP + 0.09 AnBmP + other products	
PHEN + NO3 → 0.04 AnBlP + 0.12 AnBmP + other products	

* CSL (cresol and other hydroxy substituted aromatics except phenols), CRES (cresol and higher molecular weight phenols).

3 Description of the simulations

3.1 Modeling domain and setup

The modeling domain covers western and part of eastern Europe with a horizontal resolution of $0.5° \times 0.5°$. Detailed descriptions of the modeling domain and setup are found in Kim et al. (2009) and Sartelet et al. (2007). The simulations are carried out for one month from 15 July to 15 August 2001. Meteorological inputs are obtained from a reanalysis provided by the European Centre for Medium-Range Weather Forecasts (ECMWF). Anthropogenic emissions of gases and PM were generated with the European Monitoring and Evaluation Programme (EMEP) inventory for 2001. NMHC (non-methane hydrocarbons) are disaggregated into molecular species following Passant (2002). The re-aggregation into model species is done following Carter's speciation database for both CB05 and RACM2 (Carter, 2008). As mentioned in Sect. 2.3, HC8, API and LIM were added to CB05 as model species for SVOC formation. Therefore, the speciation database of RACM2 is used to generate the emissions of HC8, API and LIM in

Table 3d. Long-chain alkane and anthropogenic alkene oxidation chemistry for SVOC formation.

RACM2	CB05
HC8[a] + HO → 0.048 AnBlP + other products	HC8[c] + OH → 0.048 AnBlP + OH[b]
OLT[a] + HO → 0.0016 AnBlP + other products	OLE[a] + OH → 0.0016 AnBlP + other products
OLT + O3 → 0.0016 AnBlP + other products	OLE + O3 → 0.0016 AnBlP + other products
OLT + NO3 → 0.0016 AnBlP + other products	OLE + NO3 → 0.0016 AnBlP + other products
OLI[a] + HO → 0.003 AnBlP + other products	IOLE[a] + OH → 0.003 AnBlP + other products
OLI + O3 → 0.003 AnBlP + other products	IOLE + O3 → 0.003 AnBlP + other products
OLI + NO3 → 0.003 AnBlP + other products	IOLE + NO3 → 0.003 AnBlP + other products

[a] HC8 (surrogate for long-chain alkanes), OLT and OLE (surrogate for terminal alkenes), OLI and IOLE (surrogate for internal alkenes).
[b] see Table 3a.
[c] new species added to the CB05 mechanism for the SVOC formation.

Table 3e. Biogenic alkene oxidation chemistry for SVOC formation.

RACM2	CB05
API[a] + HO → 0.164 BiA0D + 0.117 BiA1D + 0.076 BiA2D + other products	API[c] + OH → 0.164 BiA0D + 0.117 BiA1D + 0.076 BiA2D + OH[b]
API + NO3 → 0.8 BiBmP + other products	API + NO3 → 0.8 BiBmP + NO3[b]
API + O3 → 0.127 BiA0D + 0.142 BiA1D + 0.044 BiA2D + other products	API + O3 → 0.127 BiA0D + 0.142 BiA1D + 0.044 BiA2D + O3[b]
LIM[a] + HO → 0.407 BiA0D + 0.173 BiA1D + 0.003	LIM[c] + OH → 0.407 BiA0D + 0.173 BiA1D + 0.003
BiA2D + 0.024 BiBmP + other products	BiA2D + 0.024 BiBmP + OH[b]
LIM + NO3 → 0.309 BiA0D + 0.02 BiA1D + other products	LIM + NO3 → 0.309 BiA0D + 0.02 BiA1D + NO3[b]
LIM + O3 → 0.197 BiA0D + 0.094 BiA1D + other products	LIM + O3 → 0.197 BiA0D + 0.094 BiA1D + O3[b]
ISO + HO → 0.232 BiISO1 + 0.0288 BiISO2 + other products	ISOP + OH → 0.232 BiISO1 + 0.0288 BiISO2 + other products

[a] API (surrogate for alpha-pinene and other cyclic terpenes with one double bond), LIM (surrogate for d-limonene and other cyclic diene-terpenes).
[b] see Table 3a.
[c] see Table 3d.

CB05. For anthropogenic PM, the EMEP inventory provides yearly emissions of $PM_{2.5}$ and PM_{coarse}. These raw data are temporally, chemically and granulometrically distributed. PM_{coarse} is totally attributed to mineral dust and $PM_{2.5}$ is speciated into black carbon (20%), mineral dust (35%) and primary organic aerosol (POA, 45%). Gas-phase biogenic emissions are computed as in Simpson et al. (1999). Two-thirds of monoterpene emissions are allocated to API and one-third to LIM in RACM2. In CB05, all monoterpenes are allocated to model species TERP for the original gas-phase mechanism whereas the allocation using API and LIM is also used for SVOC formation. Sea-salt emissions are included in fine and coarse particles. The parametrization of Monahan et al. (1986) for indirect generation by bubbles is used. This parametrization is valid for diameters larger than 1.6 µm. The rate of sea-salt generation is assumed to be zero for diameters lower than 1.6 µm. The distribution of sea-salt emission between the different particulate sections is done by integrating the dry rate of sea-salt generation for mass between the section bounds. By assuming that the wet radius at 80% humidity is about 2 times the dry radius of particles (Gerber, 1985), 76% of sea-salt are emitted in our last section (2.5119 to 10 µm) and 28% in the section (0.6310 to 2.5119 µm). Following Seinfeld and Pandis (1998), sea-salt emissions are assumed to be made of 30.61% sodium, 55.04% chloride and 7.68% sulfate. For gaseous boundary conditions, daily means are extracted from outputs of the global chemistry-transport model MOZART2 run over a typical year (Horowitz et al., 2003). For PM boundary conditions, daily means are based on outputs of the Goddard Chemistry Aerosol Radiation and Transport (GOCART) model for sulfate, dust, black carbon, organic carbon and sea salt (Chin et al., 2000).

3.2 Comparisons to observations

We compared the results obtained by the simulations to observed data provided by the EMEP database. For O_3, comparisons to data can be found in Kim et al. (2009). The EMEP database also provides observed data of PM_{10}, $PM_{2.5}$ and inorganic particulate species (sulfate, nitrate and ammonium) for the year 2001. The observations are given only as 24-hour averages (hourly observations are not available for 2001). Figure 1 displays the locations of the observation stations. Details on the measurement are available at http://www.emep.int.

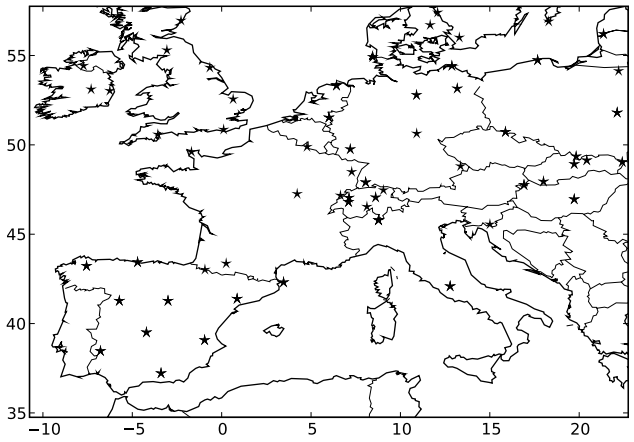

Fig. 1. Locations of the EMEP observation stations for PM.

To evaluate PM modeling, Boylan and Russell (2006) suggested to use the mean fractional bias (MFB) and the mean fractional error (MFE) defined, respectively, by

$$\mathrm{MFB} = \frac{1}{n}\sum_{i=1}^{n}\frac{c_\mathrm{i} - o_\mathrm{i}}{(c_\mathrm{i} + o_\mathrm{i})/2} \quad (1)$$

$$\mathrm{MFE} = \frac{1}{n}\sum_{i=1}^{n}\frac{|\,c_\mathrm{i} - o_\mathrm{i}\,|}{(c_\mathrm{i} + o_\mathrm{i})/2} \quad (2)$$

They proposed model performance goals (the level of accuracy that is considered to be close to the best a model can be expected to achieve) and criteria (the level of accuracy that is considered to be acceptable for modeling applications) using the MFB and the MFE. For major components of PM, the model performance goal is met when both the MFB and the MFE are less than or equal to ±30% and +50%, respectively, and the model performance criterion is met when the MFB and the MFE are less than or equal to ±60% and +75%, respectively. Table 4 summarizes the statistics obtained in the comparisons of modeled concentrations to observed data from the EMEP database. The nitrate results show the largest bias and error for both CB05 and RACM2.

The model performance goal for PM_{10} values obtained by the simulation using RACM2 is met at 17 stations among 26 stations and the model performance criterion is not met at only 6 stations. Similarly, the model performance goal for PM_{10} values obtained by the simulation using CB05 is met at 16 stations among 26 stations. The model performance criterion is mostly not met at the stations located in Spain, where the model underpredicts for both CB05 and RACM2.

Better results were obtained for $PM_{2.5}$ than for PM_{10}. The model performance goal, for both CB05 and RACM2, is met at 11 stations among 17 stations and the model performance criterion is met at all stations. Again, lower performance is obtained at the stations in Spain.

For sulfate, 24 stations and 30 stations among 54 stations meet the model performance goal for CB05 and RACM2, respectively. Only 9 stations for CB05 and 7 stations for RACM2 are out of the model performance criterion. For ammonium, better model performance is obtained than for sulfate. Six among 9 stations meet the model performance goal for both CB05 and RACM2. For nitrate, the goal is met at only 4 stations out of 14 stations for both CB05 and RACM2. However, the model performance criterion is not met at only 3 stations with CB05 and 6 stations with RACM2.

When averaged over all stations (see Table 4), the performance goal is met for all species except nitrate, for which the performance criterion is met. These results are consistent with PM model performance obtained in previous studies (Zhang et al., 2006; Bailey et al., 2007; Russell, 2008) and are, therefore, considered to be satisfactory.

4 Results

The averaged concentration of $PM_{2.5}$ over the domain is slightly higher with RACM2 than with CB05 (difference $<1\,\mu g\,m^{-3}$, 6%). Figure 2 displays domain-averaged differences of the concentrations of $PM_{2.5}$ and $PM_{2.5}$ chemical components between the two mechanisms. The concentration of inorganic $PM_{2.5}$ is higher for RACM2 than for CB05 (+16% of sulfate, +10% of ammonium and +11% of nitrate), whereas the concentration of SOA is slightly higher for CB05 than for RACM2 (+2%). The concentrations of mineral dust and POA remain unchanged when using CB05 or RACM2. Before studying the impact of using CB05 or RACM2 on particulate chemical components, we discuss the $PM_{2.5}$ chemical composition over Europe.

4.1 $PM_{2.5}$ chemical composition

Accurate measurements of aerosol chemical composition remain challenging. Inorganic species may be accurately measured with an uncertainty of about ±10% for major species (Putaud et al., 2000), except in case where significant artifacts occur for nitrate and ammonium (e.g., under warm conditions) (Hering and Cass, 1999; Keck and Wittmaack, 2005). However, measurements of organic carbon and black carbon concentrations in particles may vary from an instrumental method to another. As a result, the uncertainties in black carbon may be on the order of a factor of two and those in organic carbon can be about 20% (Chow et al., 2001).

In our study, $PM_{2.5}$ is composed on average of sulfate (25%), mineral dust (17%), nitrate (12%), SOA (13%), ammonium (11%), chloride (10%), sodium (7%), black carbon (2%) and POA (3%). Figure 3 presents the contributions of secondary chemical components to $PM_{2.5}$ over Europe using RACM2. Results obtained using CB05 are not significantly different.

Table 4. Comparison of modeled concentrations to observations from the EMEP database ($\mu g/m^3$).

	Stations	Observation[a,b]	Chemical mechanism	Modeled data[a,b]	MFB[a]	MFE[a]
PM_{10}	26	18.9	CB05	14.0	−27%	41%
			RACM2	14.8	−22%	40%
$PM_{2.5}$	17	13.6	CB05	12.7	−12%	39%
			RACM2	13.5	−7%	39%
Sulfate	54	2.9	CB05	2.5	−0.1%	45%
			RACM2	2.8	1%	45%
Nitrate	14	1.6	CB05	2.4	0%	73%
			RACM2	2.7	11%	72%
Ammonium	9	1.6	CB05	1.8	10%	43%
			RACM2	2.0	19%	45%

[a] mean values over all stations.
[b] monthly-mean concentrations

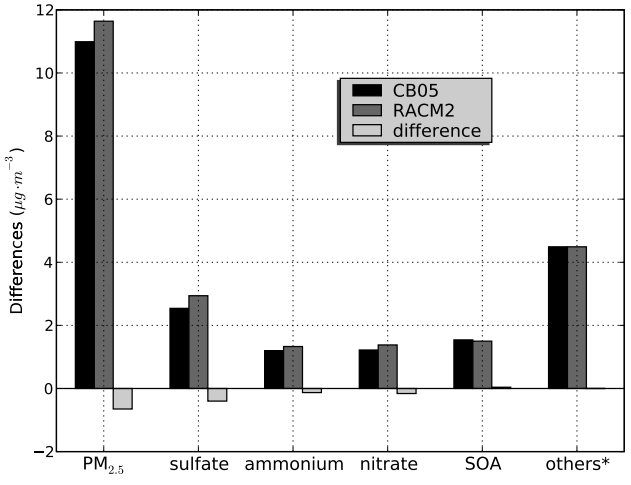

Fig. 2. Domain-averaged differences of the concentrations of $PM_{2.5}$ and $PM_{2.5}$ chemical components between the two mechanisms, CB05 and RACM2. ∗: mineral dust, black carbon, sea salts and primary organic aerosol.

Sulfate is a dominant component of $PM_{2.5}$ in marine regions. This is partly due to direct emissions of sea-salt and to the oxidation of SO_2 from ship emissions. Nitrate and ammonium are mostly formed over land in northern Europe, where emissions of NH_3 and NO_x are the largest. Ammonium is also formed over marine regions because it neutralizes particulate sulfate. Anthropogenic organic aerosols are mostly formed in large urban regions, whereas biogenic organic aerosols are formed where emissions of monoterpenes are high (northern Africa, Austria, southwestern France and Sweden) or where emissions of isoprene are high (Spain, Italy and eastern Europe).

4.2 $PM_{2.5}$ differences by species

Differences in PM concentrations between CB05 and RACM2 are mostly due to differences in oxidant concentrations. Differences in concentrations of OH and NO_3 between CB05 and RACM2 are partly due to differences in the organic chemistry formulation but also to different kinetics of oxidation of NO (Kim et al., 2009). The kinetics of oxidation of $NO + O_3 \rightarrow NO_2$ is higher in CB05 than in RACM2, whereas the kinetics of oxidation of $NO + HO_2 \rightarrow NO_2 + OH$ is higher in RACM2 than in CB05. Over the entire domain, OH and O_3 concentrations are on average higher with RACM2 (OH: 24% and O_3: 3%) but the average NO_3 concentration is higher with CB05 (17%).

4.2.1 Inorganic aerosols

The mean concentration of sulfate is higher in RACM2 than in CB05 (16%). Sulfate is formed in both the gas phase and the aqueous phase. In the gas phase, the oxidation of SO_2 by the hydroxyl radical (OH) produces sulfuric acid, which condenses to form sulfate. Because the mean concentration of OH is 24% higher in RACM2, and the kinetics of the oxidation of SO_2 is greater in RACM2 than in CB05 by 5%, the concentration of sulfate is higher in RACM2. In the aqueous phase, it is not easy to diagnose whether RACM2 or CB05 would produce more sulfate. The oxidation of SO_2 by ozone and/or hydrogen peroxide (H_2O_2) produces sulfate. O_3 is higher on average in RACM2 than CB05 (3%), whereas H_2O_2 is higher in CB05 than in RACM2 (13%). The modeling results show that gas-phase SO_2 oxidation dominates sulfate formation here.

The nitrate concentration over the entire domain is 11% higher with RACM2 than CB05. Differences in nitrate concentrations are due to differences in HNO_3 concentrations, which may condense to form nitrate. HNO_3 is produced in

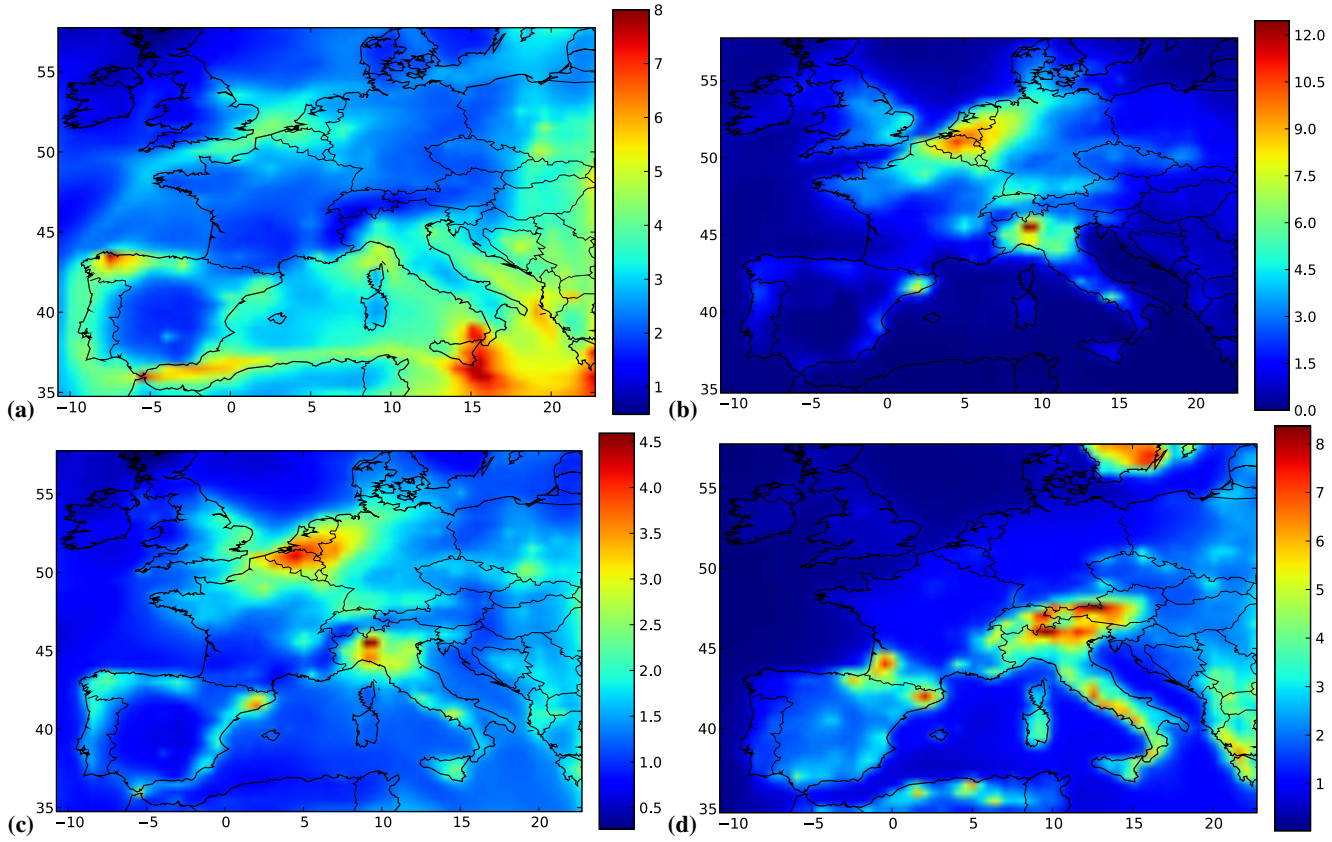

Fig. 3. Contributions (μg/m^3) of secondary chemical components to $PM_{2.5}$ over Europe: **(a)** sulfate, **(b)**nitrate, **(c)** ammonium, **(d)** SOA.

the gas phase, the aqueous phase, as well as heterogeneously on particle and droplet surfaces. The following gas-phase reaction is the dominant daytime source:

$$NO_2 + OH \rightarrow HNO_3 \quad (3)$$

and the main nighttime sources are the NO_3 and N_2O_5 heterogeneous reactions:

$$NO_3 + NO_2 \rightarrow N_2O_5 \quad (4)$$

$$N_2O_5 + H_2O \rightarrow 2HNO_3 \quad (5)$$

$$NO_3 + H_2O \rightarrow HNO_3 + OH \quad (6)$$

Differences in the production of HNO_3 from the oxidation of NO_2 by OH are mostly due to differences in OH concentrations, because the concentration of NO_2 is similar in RACM2 and CB05 (average difference 1%). The difference in the kinetics of the oxidation of NO_2 by OH between the two mechanisms is small (3%). The formation of HNO_3 by heterogeneous reactions is higher with CB05 because of the higher concentration of NO_3 (17%). However, the contribution of the heterogeneous reactions to the formation of HNO_3 is not significant (3% only) compared to the gas-phase formation in this study.

Ammonium is produced by the condensation of NH_3 on particles, mostly via neutralization of sulfate and formation of ammonium nitrate. As shown in Sartelet et al. (2007), ammonium nitrate formation over Europe is limited by the formation of HNO_3. Because the HNO_3 concentration is higher on average in RACM2 than in CB05, the ammonium nitrate formation is enhanced in RACM2. The combination of higher sulfate and HNO_3 concentrations leads to higher ammonium concentrations with RACM2 (+10%).

4.2.2 Secondary organic aerosols

Monthly-mean concentrations of SOA are not considerably different between the two mechanisms. The mean difference is 2% over the entire domain and the average value of the concentration of SOA in CB05 is higher than in RACM2 by only 0.04 μg m^{-3}. The maximum of the local differences between the two mechanisms is 0.6 μg m^{-3} at locations where SOA concentrations predicted by CB05 are higher and 0.8 μg m^{-3} at locations where SOA concentrations predicted by RACM2 are higher.

CB05 and RACM2 have the same emissions and photochemical reaction rates of gaseous biogenic VOC for monoterpenes (see Sect. 2.3). Therefore, differences in the

particulate phase for monoterpenes come from differences in the concentrations of oxidants (OH, O_3 and NO_3). RACM2 produces more OH (24%) and O_3 (3%) than CB05 whereas CB05 produces more NO_3 (17%) than RACM2. Because the formation of the hydrophilic monoterpene SVOC depends on OH and O_3, their concentration is mostly higher in RACM2 than in CB05 (BiA1D: 5% and BiA2D: 7%). The concentration of BiA0D is higher in CB05 than in RACM2. The reaction of LIM with NO_3 is the main reaction for the formation of BiA0D at nighttime. The higher concentration of NO_3 in CB05 leads to the higher concentration of BiA0D in CB05. However, the concentration of BiAOD is very low compared to those of BiA1D and BiA2D. The reaction of API with NO_3 produces a hydrophobic monoterpene SVOC: BiBmP. The concentration of BiBmP is higher in CB05 than in RACM2 (8%), because of the higher NO_3 concentration in CB05.

The contribution of isoprene to the formation of SOA is important in both mechanisms (about 25% of the monthly-mean concentration of SOA). The kinetics of the isoprene oxidation by OH is almost the same in RACM2 and in CB05 (1% difference). Therefore, the difference in OH concentrations is the main cause of the difference in isoprene SOA concentrations in the particulate phase. RACM2 is more conducive to the formation of isoprene SVOC than CB05 (differences for BiISO1: 6% and BiISO2: 7%) because of higher concentration of OH (24%).

The production of anthropogenic SVOC is more important with CB05 than with RACM2, although OH concentration is lower in CB05. The difference between CB05 and RACM2 originates from the modeling of the reaction of aromatic-OH adducts with O_2 in the gas phase. Aromatic-OH adducts react with O_2 to either abstract an H atom to form ring-retaining products (cresol; via the oxidation of toluene) or add O_2 to form a peroxyl radical that subsequently leads to ring opening and the formation of scission products. RACM2 assumes that the majority of this reaction leads to ring-opening products (dicarbonyls and epoxide). In contrast, CB05 has a high fraction of ring-retaining products (cresol). Figure 4 presents the differences of monthly-mean concentrations of cresol between CB05 and RACM2 at each grid point. The mean concentration of cresol in RACM2 is only 20% of that in CB05. Higher concentration of cresol in CB05 results in higher concentrations of the two hydrophobic SVOC (AnBlP: 9% and AnBmP: 40%) in CB05 than in RACM2. If the formation of these SVOC by cresol oxidation is removed from the two mechanisms, the differences in AnBlP and AnBmP concentrations become much lower (AnBlP: 3% and AnBmP: 0.3%).

The mean concentration of toluene is higher with CB05 than with RACM2 (16%), because the emission rate of TOL (model species for toluene) is higher in CB05 (10%). When volatile organic compound (VOC) emissions are allocated to model species, each mechanism uses different methods for the VOC aggregation, leading to different emission rates

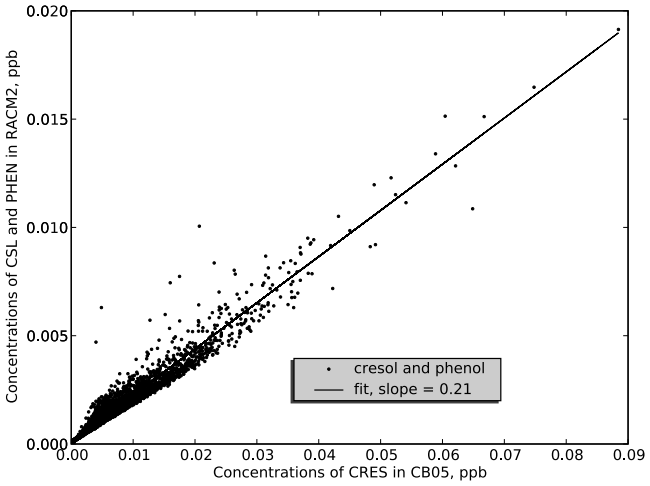

Fig. 4. Relation of concentrations of cresol between CB05 and RACM2 at each location. The concentration of phenol that is specified only in RACM2 is added to the concentration of cresol for RACM2.

(e.g., benzaldehydes are explicitly represented by BALD model species in RACM2, however, they are represented by TOL in CB05).

PAMGLY, another anthropogenic aerosol is formed from methylglyoxal (MGLY) in the aqueous phase by oligomerization. PAMGLY concentration depends only on MGLY concentration because the coefficient of gas/particle partition for methylglyoxal is assumed to already include the effect of oligomerization (Debry et al., 2007b). Because the kinetics of the oxidation of MGLY by OH is higher in CB05 than in RACM2 at 298 K (13%), the concentration of MGLY is higher in RACM2 than in CB05 (11%). Therefore, the concentration of PAMGLY in RACM2 is higher than in CB05 (20%). Similarly, PAGLY is formed from glyoxal (GLY) by oligomerization. GLY is only included in RACM2. The concentrations of PAMGLY and PAGLY are low compared with other anthropogenic aerosols and they have, therefore, little influence on SOA total concentrations.

4.3 $PM_{2.5}$ spatial distributions

Figure 5 presents the modeled $PM_{2.5}$ concentrations over Europe for RACM2 and the differences between CB05 and RACM2. For the two chemical mechanisms, high concentrations of $PM_{2.5}$ are simulated over large urban areas (e.g. Antwerp, Barcelona, Cologne, Milan and Paris) and over northern Africa (due to mineral dust) by both CB05 and RACM2 ($>20\,\mu g\,m^{-3}$). RACM2 overall predicts more $PM_{2.5}$ than CB05 except in cities such as Paris and Madrid where the formation of nitrate, ammonium and SOA with CB05 is higher than with RACM2. The differences are large over northern Italy, part of the Mediterranean Sea and Barcelona in Spain ($>1.5\,\mu g\,m^{-3}$).

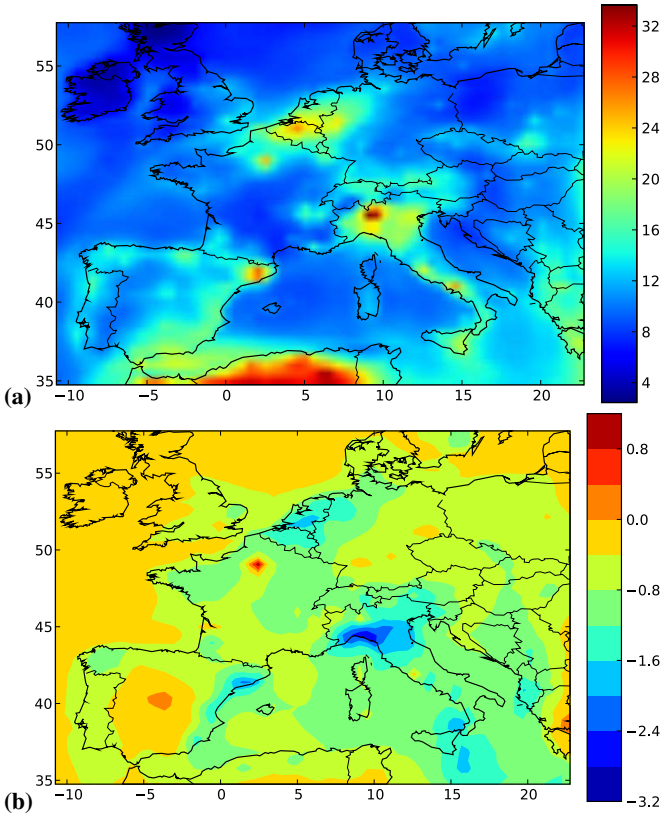

Fig. 5. Modeled $PM_{2.5}$ concentrations ($\mu g/m^3$) over Europe with **(a)** RACM2 and **(b)** the corresponding differences between the two mechanisms (CB05 – RACM2).

4.3.1 Inorganic aerosols

Figure 6 presents the differences of the secondary $PM_{2.5}$ chemical components between CB05 and RACM2. Monthly-mean concentrations of sulfate are higher with RACM2 than CB05. The difference is particularly high over the Mediterranean Sea and northwestern Spain. The differences are due to the oxidation of SO_2 by OH in the gas-phase as explained in Sect. 4.2.1. In these regions, high SO_2 emissions from marine traffic combine with high OH concentrations. OH concentrations are higher in RACM2 than in CB05, for example, the monthly-mean concentration of OH is about 50% and 25% higher in RACM2 than CB05 over the Adriatic Sea and northwestern Spain, respectively.

For nitrate, differences of monthly-mean concentrations are large in Paris, Barcelona, the Netherlands and northern Italy. In Paris, a higher concentration of nitrate is obtained with CB05. However, in Barcelona, northern Italy and the Netherlands, higher concentrations of nitrate are obtained with RACM2.

The formation of nitrate is limited by one of the two following precursors: ammonia or HNO_3. To diagnose the limiting precursor for the formation of nitrate, the following "Gas Ratio" indicator (GR) may be used:

$$GR = \frac{[NH_3^T] - 2[SO_4^{2-}]}{[HNO_3^T]}, \quad (7)$$

where NH_3^T (total ammonia) is the sum of ammonium and ammonia and HNO_3^T (total HNO_3) is the sum of nitrate and HNO_3 (Ansari and Pandis, 1998; Park et al., 2004). Figure 7 shows the simulated monthly-mean GR over Europe. As discussed by Sartelet et al. (2007), over continental Europe, nitrate formation is limited by the formation of HNO_3 ($GR > 1$). Ammonia limits nitrate formation over the English Channel, the North Sea and part of the Mediterranean Sea ($0 < GR < 1$). Negative GR values, which indicate an acidic sulfate aerosol, are limited to the southern Mediterranean Sea where there is high marine traffic and, therefore, high SO_2 emissions.

In Paris, Barcelona, northern Italy and the Netherlands, the nitrate concentration varies with the HNO_3 concentration ($GR > 1$). As the total HNO_3 concentration is higher with CB05 than RACM2 over Paris, the nitrate concentration is higher with CB05. However, over the rest of continental Europe, and specially over Barcelona, northern Italy and the Netherlands where the nitrate concentration is high, the nitrate concentration is lower with CB05 than RACM2 because the total HNO_3 concentration is lower. Over the North Sea, the Atlantic Ocean and the English Channel, the nitrate concentrations are low but higher with CB05 than RACM2. These higher concentrations of nitrate with CB05 are linked to higher concentrations of free ammonia under ammonia-limited condition ($0 < GR < 1$), which are itself due to lower concentrations of sulfate with CB05.

Over continental Europe, because $GR > 1$, differences of ammonium monthly-mean concentration follow the same pattern as nitrate concentration (e.g. high differences in Paris, Barcelona, the Netherlands and northern Italy).

4.3.2 Secondary organic aerosols

The regions where high differences of SOA concentrations between CB05 and RACM2 are obtained, are well correlated with the regions where high SOA concentrations are obtained. Higher SOA concentrations are predicted by CB05 over most of Europe except Sweden, northern Africa, southwestern France and Austria. SOA concentrations are particularly higher with CB05 over parts of Italy, Spain and Greece.

The higher SOA concentrations with RACM2 over Sweden, northern Africa, southwestern France and Austria are due to higher SOA concentrations formed from monoterpene SVOC (BiA0D, BiA1D, BiA2D and BiBmP). In these regions, the concentrations of these SOA are high and as the concentrations increase, the differences of the concentrations

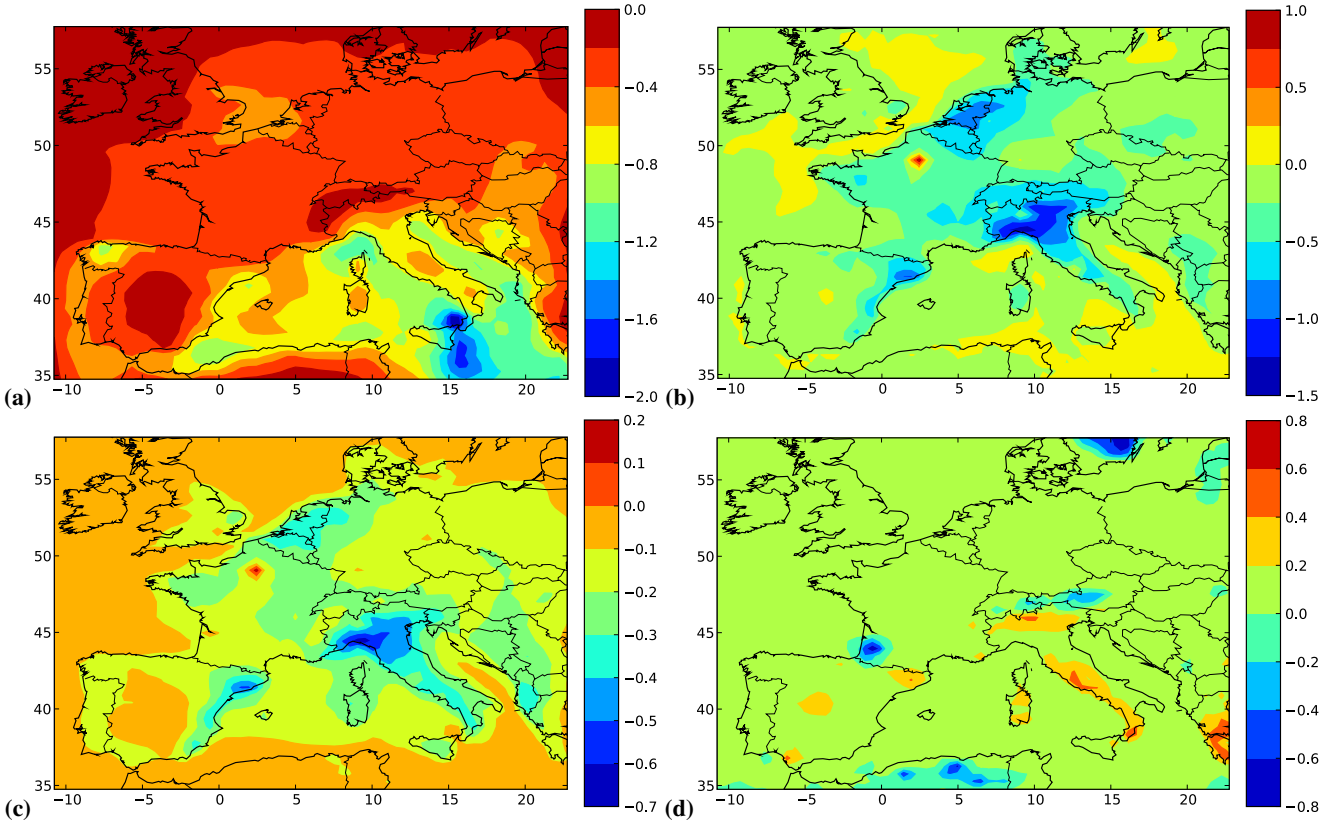

Fig. 6. Differences (CB05 – RACM2, μg m^{-3}) of $PM_{2.5}$ chemical components over Europe: **(a)** sulfate, **(b)** nitrate, **(c)** ammonium, **(d)** SOA.

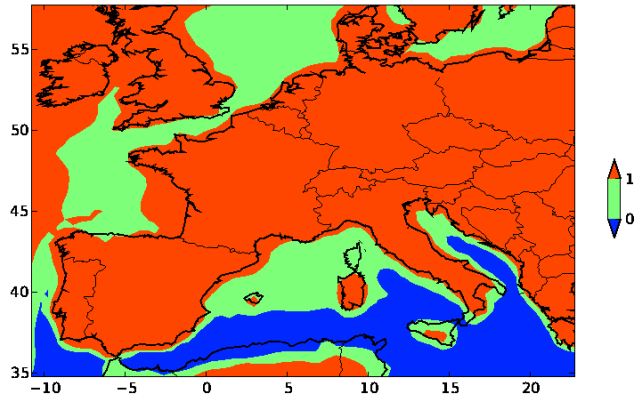

Fig. 7. Monthly-mean gas ratio (GR) in summer 2001 over Europe. GR < 0: acidic sulfate aerosol (blue), 0 < GR < 1: nitrate formation limited by ammonia (green), GR > 1: nitrate formation limited by HNO_3 (orange).

also increase. The formation of the hydrophilic monoterpene SVOC (BiA0D and BiA1D) depends on the concentrations of OH and O_3. The concentration of the hydrophobic monoterpene SVOC (BiBmP) depends on the concentration of NO_3. In these regions, the concentrations of OH, O_3 and NO_3 tend to be higher with RACM2 than CB05. Therefore, the concentration of SOA is higher with RACM2 than CB05.

The concentrations of SOA formed from the anthropogenic SVOC are higher in CB05 than in RACM2 over the whole Europe because the concentration of the anthropogenic precursors are higher with CB05 than RACM2.

The higher SOA concentrations with CB05 in Italy, Spain and Greece are due to higher concentrations of SOA formed from the monoterpene SVOC (BiBmP) and the isoprene SVOC (BiISO1 and BiISO2). The differences of SOA formed from monoterpenes SVOC (BiBmP) are higher with CB05 because NO_3 concentrations are higher.

Differences of SOA concentrations formed from the two isoprene SVOC show different patterns. Figure 8 presents the differences of SOA formed from the isoprene SVOC (BiISO1 and BiISO2) between CB05 and RACM2. In Italy, Greece and Spain, the concentrations of SOA formed from BiISO1 are higher with CB05. However, in the same regions, the concentrations of SOA formed from BiISO2 are higher with RACM2. BiISO1 and BiISO2 have the same dependence on oxidant concentration. Differences are due to differences in gas/particle phase partitioning. The partitioning depends on the concentration of primary and secondary organics of PM, as follows Pankow (1994a,b)

$$[A] \simeq K[G][\mathrm{OM}] \tag{8}$$

where K is the phase partitioning coefficient (m^3/μg), [OM]

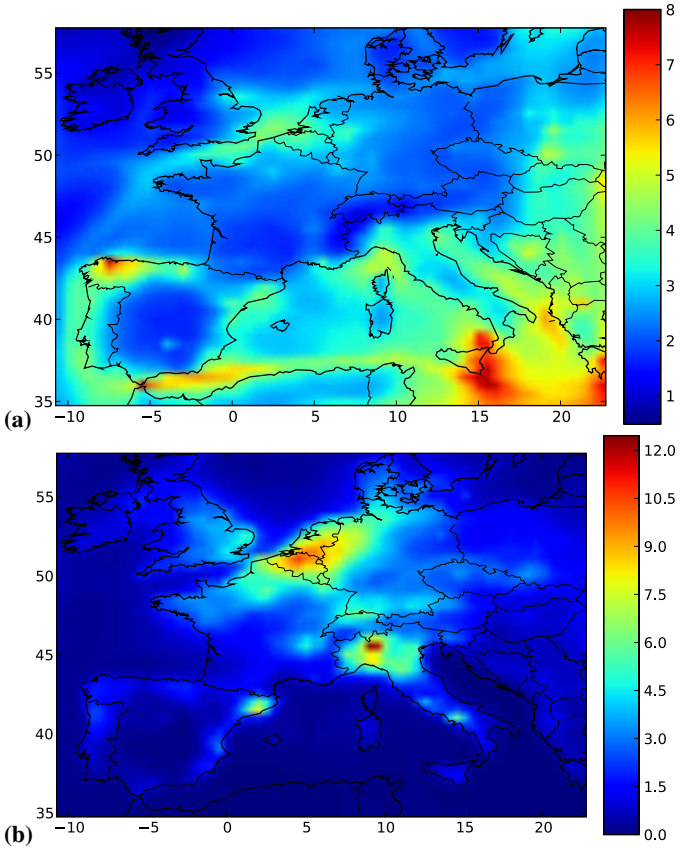

Fig. 8. Differences (CB05 – RACM2, $\mu g\,m^{-3}$) of SOA formed from **(a)** BiISO1 and **(b)** BiISO2 over Europe.

is the total organic mass (primary and secondary) ($m^3/\mu g$), $[A]$ is the concentration of the organic species in the particulate phase ($\mu g/m^3$) and $[G]$ is the concentration of the organic species in the gas phase ($\mu g/m^3$). In Italy, Greece and Spain, the organic mass ([OM]) is higher with CB05 (see Fig. 6) because of higher BiBmP concentrations, which are due to higher NO_3 concentrations. However, gaseous SVOC (BiISO1 and BiISO2) are lower with CB05 because of lower OH concentrations. The compensating negative differences of $[G]$ and positive differences of [OM] lead to variable differences in particulate concentrations, $[A]$ that tend to be positive when the partitioning coefficient K is low (case of BiISO1) and negative when it is high (case of BiISO2).

5 Conclusions

The impact of two chemical mechanisms, CB05 and RACM2, on the formation of secondary inorganic and organic aerosols was studied using the air quality model, Polair3D of the Polyphemus modeling platform. The monthly-mean concentration of $PM_{2.5}$ over the domain is higher with RACM2 than CB05 by 6%. This difference is due to inorganic aerosols (sulfate, ammonium and nitrate) and organic aerosols (biogenic and anthropogenic).

Differences in inorganic aerosols result primarily from differences in OH concentrations. The monthly-mean difference for sulfate is 16% and the maximum local difference is 29%. For nitrate, the difference of monthly-mean concentrations is 11% and the maximum local difference is 51%. For ammonium, the difference of monthly-mean concentrations is 10% and the maximum local difference is 23%. Nitrate formation is limited by the formation of HNO_3 over continental Europe. However, ammonia limits nitrate formation over the English Channel, the North Sea and part of the Mediterranean Sea. In other words, differences in the concentrations of nitrate are mostly due to differences in the concentrations of HNO_3 where the concentrations of ammonia are high, whereas differences in the concentrations of ammonia, which are due to differences in the concentrations of sulfate, result in differences in the formation of nitrate where the concentration of HNO_3 is high relative to ammonia.

Differences in organic aerosols result also mostly from differences in oxidant concentrations (OH, O_3 and NO_3). The difference in monthly-mean concentrations of anthropogenic SOA is 22%. Most of that difference is due to aromatic SOA. Differences in the contribution of aromatics to anthropogenic aerosol formation are due to the fact that aromatics oxidation in CB05 leads to more cresol formation from toluene oxidation. The concentration of SOA formed by the cresol oxidation is very different between CB05 and RACM2. The maximum local differences are 40% for aerosol formed from AnBIP and 115% for aerosol formed from AnBmP.

The difference in monthly-mean concentrations of biogenic SOA is 1%, which is the compensating difference of higher concentrations of BiBmP with CB05 (+12%) and lower concentrations of the other biogenic SOA (−4%). Differences in the biogenic aerosol formation are partly due to differences in oxidant concentrations and partly to the total organic mass, which influences the formation of biogenic aerosol by gas-particle partitioning coefficients. The maximum local differences of aerosol formed from monoterpene SVOC are 12% (BiA0D), 52% (BiA1D), 45% (BiA2D) and 91% (BiBmP). For the aerosol formed from isoprene SVOC, the maximum local differences are 21% (BiISO1) and 16% (BiISO2).

The results obtained in this comparison of CB05 and RACM2 on the formation of secondary aerosols show that the predictions of $PM_{2.5}$ with the mechanisms are very similar (only 6% difference and 15% maximum local difference). Differences may be higher for specific compounds (nitrate, AnBmP and BiBmP). Besides, the highest difference, which is obtained for anthropogenic aerosols (aromatics oxidation), could be partly solved by updating CB05 with CB05-TU, a chemical mechanism in which the toluene oxidation mechanism was recently improved (Whitten et al., 2010). The concentration of cresol is lower with CB05-TU than with

CB05 by about 70%. Thus, the discrepancy in aromatics SOA formation between CB05 and RACM2 would be significantly reduced with CB05-TU.

The effects of a gas-phase chemical kinetic mechanism for ozone formation on SOA concentrations can be classified into three main categories: (1) direct effects that result from the design of the mechanism leading to different yields of SOA precursors (e.g., different precursor emissions due to different aggregation of molecular VOC species into VOC surrogate model species, different kinetics of VOC oxidation, different stoichiometric coefficients for VOC oxidation products such as different cresol yields in RACM2 and CB05), (2) primary indirect effects due to different concentrations of the oxidant species (OH, O_3 and NO_3), which affect the rate of oxidation of VOC species and (3) secondary indirect effects due to interactions among SOA species (e.g., an increase in one SOA species leads to greater organic particulate mass available for additional absorption of other SOA species).

Here, a harmonized approach was used when modifying the two mechanisms to handle SOA formation. Early treatment of SOA formation in air quality models used simple approaches where SOA formation was treated at the first oxidation step of the precursor species and only a few mechanisms have treated SOA formation at later oxidation steps Griffin et al. (2002). We have attempted to reflect the current understanding of SOA formation by accounting for the NO_x-regime dependence of SOA formation from aromatic compounds and treating SOA formation at later oxidation steps. Accordingly, the future development of mechanisms for SOA formation will require chemical mechanisms that can account for the various gas-phase reaction steps that are important for SOA formation.

Acknowledgements. We thank Deborah Luecken (US Environmental Protection Agency) and Gookyoung Heo (University of Texas, Austin) for helpful discussions about CB05. We also thank Wendy Goliff (University of California, Riverside) and William Stockwell (Howard University) for useful discussions about RACM2.

Edited by: R. Harley

References

Ansari, A. S. and Pandis, S. N.: Response of inorganic PM to precursor concentrations, Environ. Sci. Technol., 32, 2706–2714, doi:10.1021/es971130j, 1998.

Bailey, E., Gautney, L., Kelsoe, J., Jacobs, M., Mao, Q., Condrey, J., Pun, B., Wu, S.-Y., Seigneur, C., Douglas, S., Haney, J., and Kumar, N.: A comparison of the performance of four air quality models for the Southern Oxidants Study episode in July 1999, J. Geophys. Res., 112, D05306, doi:10.1029/2007JD008675, 2007.

Boylan, J. W. and Russell, A. G.: PM and light extinction model performance metrics, goals, and criteria for three-dimensional air quality models, Atmos. Environ., 40, 4946–4959, doi:10.1016/j.atmosenv.2005.09.087, 2006.

Carter, W. P. L.: Implementation of the SAPRC-99 chemical mechanism into the models- 3 framework, report to the United States Environmental Protection Agency, available at: http://www.cert.ucr.edu/~carter/pubs/s99mod3.pdf, 2000.

Carter, W. P. L.: Development of an improved chemical speciation database for processing emissions of volatile organic compounds for air quality models, available at: http://www.engr.ucr.edu/~carter/emitdb/, 2008.

Carter, W. P. L.: Development of the SAPRC-07 chemical mechanism and updated ozone reactivity scales, report to the California Air Resources Board, available at: http://www.engr.ucr.edu/~carter/SAPRC/saprc07.pdf, 2010.

Chin, M., Rood, R. B., Lin, S.-J., Müller, J.-F., and Thompson, A. M.: Atmospheric sulfur cycle simulated in the global model GOCART: Model description and global properties, J. Geophys. Res., 105, 24671–24687, 2000.

Chow, J. C., Watson, J. G., Crow, D., Lowenthal, D. H., and Merrifield, T.: Comparison of IMPROVE and NIOSH carbon measurements, Aerosol Sci. Technol., 34, 23–34, doi:10.1080/02786820119073, 2001.

Debry, É., Fahey, K., Sartelet, K., Sportisse, B., and Tombette, M.: Technical Note: A new SIze REsolved Aerosol Model (SIREAM), Atmos. Chem. Phys., 7, 1537–1547, doi:10.5194/acp-7-1537-2007, 2007a.

Debry, É., Seigneur, C., and Sartelet, K.: Organic aerosols in the air quality platform Polyphemus: oxidation pathways, hydrophilic/hydrophobic partitioning and oligomerization, International Aerosol Modeling Algorithms, University of California, Davis, 2007b.

Finlayson-Pitts, B. J. and Pitts Jr., J. N.: Chemistry of the upper and lower atmosphere, Academic Press, San Diego, 2000.

Gerber, H.: Relative-humidity parameterization of the Navy Aerosol Model (NAM), technical Report 8956, Natl. Res. Lab., Washington DC, 1985.

Gery, M. W., Whitten, G. Z., Killus, J. P., and Dodge, M. C.: A photochemical kinetics mechanism for urban and regional scale computer modeling, J. Geophys. Res., 94(D10), 12925–12956, 1989.

Goliff, W. S. and Stockwell, W. R.: The Regional Atmospheric Chemistry Mechanism, version 2, an update, International conference on Atmospheric Chemical Mechanisms, University of California, Davis, 2008.

Goliff, W. S. and Stockwell, W. R.: The Regional Atmospheric Chemistry Mechanism, version 2. 1. Description and Evaluation, J. Geophys. Res., submitted, 2010.

Griffin, R. J., Dabdub, D., and Seinfeld, J. H.: Secondary organic aerosol 1. Atmospheric chemical mechanism for production of molecular constituents, J. Geophys. Res., 107(D17), doi:10.1029/ 2001JD000541, 2002.

Hering, S. and Cass, G.: The magnitude of bias in the measurement of $PM_{2.5}$ arising from volatilization of particulate nitrate from teflon filters, J. Air Waste Manage., 49, 725–733, 1999.

Horowitz, L. W., Walters, S., Mauzerall, D. L., Emmons, L. K., Rasch, P. J., Granier, C., Tie, X., Lamarque, J.-F., Schultz, M. G., Tyndall, G. S., Orlando, J. J., and Brasseur, G. P.: A global simulation of tropospheric ozone and related tracers: Description and evaluation of MOZART, version 2, J. Geophys. Res., 108, 4784,

doi:10.1029/2002JD002853, 2003.

Jacob, D. J.: Heterogeneous chemistry and tropospheric ozone, Atmos. Environ., 34, 2131–2159, doi:10.1016/S1352-2310(99)00462-8, 2000.

Keck, L. and Wittmaack, K.: Effect of filter type and temperature on volatilisation losses from ammonium salts in aerosol matter, Atmos. Environ., 39, 4093–4100, doi:10.1016/j.atmosenv.2005.03.029, 2005.

Kim, Y., Sartelet, K., and Seigneur, C.: Comparison of two gas-phase chemical kinetic mechanisms of ozone formation over Europe, J. Atmos. Chem., 62, 89–119, doi:10.1007/s10874-009-9142-5, 2009.

Luecken, D. J.: Comparison of atmospheric chemical mechanisms for regulatory and research applications, in: Simulation and Assessment of Chemical Processes in a Multiphase Environment, Springer, Netherlands, 95–106, doi:10.1007/978-1-4020-8846-9_8, 2008.

Mallet, V., Quélo, D., Sportisse, B., Ahmed de Biasi, M., Debry, É., Korsakissok, I., Wu, L., Roustan, Y., Sartelet, K., Tombette, M., and Foudhil, H.: Technical Note: The air quality modeling system Polyphemus, Atmos. Chem. Phys., 7, 5479–5487, doi:10.5194/acp-7-5479-2007, 2007.

Monahan, E. C., Spiel, D. E., and Davidson, K. L.: A model of marine aerosol generation via whitecaps and wave disruption, in: Oceanic Whitecaps and their role in air-sea exchange processes, 167–174, D. Reidel, Netherlands, 1986.

Nenes, A., Pandis, S. N., and Pilinis, C.: ISORROPIA: A new thermodynamic equilibrium model for multiphase multicomponent inorganic aerosols, Aquat. Geochem., 4, 123–152, doi:10.1023/A:1009604003981, 1998.

Ng, N. L., Kroll, J. H., Chan, A. W. H., Chhabra, P. S., Flagan, R. C., and Seinfeld, J. H.: Secondary organic aerosol formation from m-xylene, toluene, and benzene, Atmos. Chem. Phys., 7, 3909-3922, doi:10.5194/acp-7-3909-2007, 2007.

Pan, Y., Zhang, Y., and Sarwar, G.: Impact of gas-phase chemistry on WRF/CHEM predictions of O_3 and $PM_{2.5}$: Mechanism implementation and comparative evaluation, 7th annual CMAS conference, Chapel Hill, North Carolina, 2008.

Pankow, J. F.: An absorption model of gas/particle partitioning of organic compounds in the atmosphere, Atmos. Environ., 28, 185–188, doi:10.1016/1352-2310(94)90093-0, 1994a.

Pankow, J. F.: An absorption model of the gas/aerosol partitioning involved in the formation of secondary organic aerosol, Atmos. Environ., 28, 189–193, doi:10.1016/1352-2310(94)90094-9, 1994b.

Park, R. J., Jacob, D. J., Field, B. D., Yantosca, R. M., and Chin, M.: Natural and transboundary pollution influences on sulfate-nitrate-ammonium aerosols in the United States: Implications for policy, J. Geophys. Res., 109, D15204, doi:10.1029/2003JD004473, 2004.

Passant, N.: Speciation of UK emissions of NMVOC, AEA Technology, AEAT/ENV/0545, 2002.

Pun, B. K. and Seigneur, C.: Investigative modeling of new pathways for secondary organic aerosol formation, Atmos. Chem. Phys., 7, 2199–2216, doi:10.5194/acp-7-2199-2007, 2007.

Pun, B. K., Griffin, R. J., Seigneur, C., and Seinfeld, J. H.: Secondary organic aerosol 2. Thermodynamic model for gas/particle partitioning of molecular constituents, J. Geophys. Res., 107, 4333, doi:10.1029/2001JD000542, 2002.

Pun, B. K., Seigneur, C., and Lohman, K.: Modeling secondary organic aerosol formation via multiphase partitioning with molecular data, Environ. Sci. Technol., 40, 4722–4731, doi:10.1021/es0522736, 2006.

Putaud, J.-P., van Dingenen, R., Mangoni, M., Virkkula, A., Raes, F., Maring, H., Prospero, J. M., Swietlicki, E., Berg, O. H., Hillamo, R., and Mäkelä, T.: Chemical mass closure and assessment of the origin of the submicron aerosol in the marine boundary layer and the free troposphere at Tenerife during ACE-2, Tellus B, 52, 141–168, doi:10.1034/j.1600-0889.2000.00056.x, 2000.

Putaud, J.-P., van Dingenen, R., Alastuey, A., Bauer, H., Birmili, W., Cyrys, J., Flentje, H., Fuzzi, S., Gehrig, R., Hansson, H., Harrison, R., Herrmann, H., Hitzenberger, R., Hüglin, C., Jones, A., Kasper-Giebl, A., Kiss, G., Kousa, A., Kuhlbusch, T., Löschau, G., Maenhaut, W., Molnar, A., Moreno, T., Pekkanen, J., Perrino, C., Pitz, M., Puxbaum, H., Querol, X., Rodriguez, S., Salma, I., Schwarz, J., Smolik, J., Schneider, J., Spindler, G., ten Brink, H., Tursic, J., Viana, M., Wiedensohler, A., and Raes, F.: A European aerosol phenomenology - 3: Physical and chemical characteristics of particulate matter from 60 rural, urban, and kerbside sites across Europe, Atmos. Environ., 44, 1308–1320, doi:10.1016/j.atmosenv.2009.12.011, 2010.

Russell, A. G.: EPA Supersites program-related emissions-based particulate matter modeling: initial applications and advances, J. Air Waste Manage., 58, 289–302, doi:10.3155-1047-3289.58.2.289, 2008.

Sartelet, K. N., Debry, É., Fahey, K., Roustan, Y., Tombette, M., and Sportisse, B.: Simulation of aerosols and gas-phase species over Europe with the Polyphemus system: Part I – Model-to-data comparison for 2001, Atmos. Environ., 41, 6116–6131, doi:10.1016/j.atmosenv.2007.04.024, 2007.

Sarwar, G., Luecken, D., Yarwood, G., Whitten, G. Z., and Carter, W. P. L.: Impact of an updated carbon bond mechanism on predictions from the CMAQ modeling system: Preliminary assessment, J. Appl. Meteor. Climatol., 47, 3–14, 2008.

Seinfeld, J. and Pandis, S.: Atmospheric Chemistry and Physics: From Air Pollution to Climate Change, Wiley-Interscience, New York, 1998.

Simpson, D., Winiwarter, W., Börjesson, G., Cinderby, S., Ferreiro, A., Guenther, A., Hewitt, C. N., Janson, R., Aslam, M., Khalil, K., Owen, S., Pierce, T. E., Puxbaum, H., Shearer, M., Skiba, U., Steinbrecher, R., Tarrasón, L., and Öquist, M. G.: Inventorying emissions from nature in Europe, J. Geophys. Res., 104, 8113–8152, 1999.

Stockwell, W. R., Kirchner, F., Kuhn, M., and Seefeld, S.: A new mechanism for regional atmospheric chemistry modeling, J. Geophys. Res., 102, 25847–25879, 1997.

Whitten, G. Z., Heo, G., Kimura, Y., McDonald-Buller, E., Allen, D. T., Carter, W. P., and Yarwood, G.: A new condensed toluene mechanism for Carbon Bond: CB05-TU, Atmos. Environ., 44, 5346–5355, doi:10.1016/j.atmosenv.2009.12.029, 2010.

Yarwood, G., Rao, S., Yocke, M., and Whitten, G.: Updates to the Carbon Bond Chemical Mechanism: CB05 Final Report to the US EPA, RT-0400675, available at: http://www.camx.com/publ/pdfs/CB05_Final_Report_120805.pdf, 2005.

Zhang, Y., Liu, P., Queen, A., Misenis, C., Pun, B., Seigneur, C., and Wu, S.-Y.: A comprehensive performance evaluation of MM5-CMAQ for the Summer 1999 Southern Oxidants Study episode–Part II: Gas and aerosol predictions, Atmos. Environ., 40, 4839–4855, doi:10.1016/j.atmosenv.2005.12.048, 2006.

Zhang, Y., Huang, J.-P., Henze, D. K., and Seinfeld, J. H.: Role of isoprene in secondary organic aerosol formation on a regional scale, J. Geophys. Res., 112, D20207, doi:10.1029/2007JD008675, 2007.